On Pattern Transfer in Replica Molding

Ovidiu D. Gordan,[†] Bo N. J. Persson,[‡] Claudia M. Cesa,[†,§] Dirk Mayer,[†] Bernd Hoffmann,[†]
Sabine Dieluweit,[†] and Rudolf Merkel*,[†]

IBN, Research Centre Jülich, 52425 Jülich, Germany, and IFF, Research Centre Jülich, 52425 Jülich, Germany

Nano- and micromolding of elastic materials produces smoothed replicas of the mold structures. This limits the technique's resolution. Here we identified surface tension as the cause of smoothing and derived explicit equations for calculating molded feature shapes. The characteristic length scale for smoothing is given by the ratio of the interface tension to Young's modulus of the molded material. This approach offers the possibility to correct for the smoothing caused by surface tension during mold design. Moreover, it can be exploited to measure interface tension.

Introduction

Reproduction by molding is an attractive low-cost technology for the parallel production of nano- and microstructures. Molding can be realized by cross-linking silicones in a mold as is routinely done in the production of microfluidic devices[1] or stamps for microcontact printing.[2] Similarly, hot embossing[3] and nanoimprinting[4,5] are widely used technologies where polymer materials are shaped in a mold. In all of these techniques, the choice of the polymer is decisive for a faithful reproduction of the mold structure. In soft replica molding (i.e., molding in a silicone elastomer), the shape fidelity of replicas is increased by increasing the stiffness of the elastomer. An example of the effect of material stiffness can be found in Figure 1.

Here we argue that the ultimate resolution limit for molding a general shape is set by the interplay between material elasticity and interface tension because smoothing by interface tension will occur even for a material that filled the mold perfectly. In an earlier related study, Hui and co-workers treated the effect of interface tension on sharp corners in PDMS and found rounding with a radius of curvature given by the ratio of surface tension to Young's modulus.[6] Please note that smoothing by the interplay of elastic deformation and surface tension results in equilibrium shapes. In contrast to this, the interplay of surface tension and viscous flow controls the shape fidelity in producing structures via nanoimprint lithography[7] as well as in the fading of these imprints during material melting.[8] In nanoimprint lithography, shape stability is achieved upon cooling the sample well below the glass temperature (i.e., these material shapes are not in thermal equilibrium). In the following text, we will use the equilibrium nature of replicas produced via molding to derive explicit equations for the final shapes.
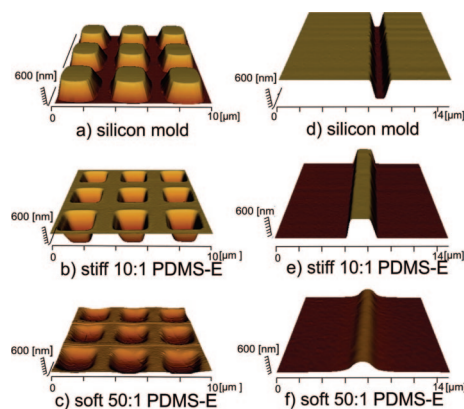
Figure 1. (a, d) Scanning force microscopy (AFM) images of SiO_2 molds and (b, e) stiff (1.6 MPa) and (c, f) soft (17 kPa) PDMS elastomer (PDMS-E) replicas.

Theoretical Considerations. The physical essence of equilibrium smoothing by an interplay between elastic and surface energy can be understood from the scaling of elastic deformation energy with volume and surface energy with surface area. Thus, at length scales below γ/Y, with Y being the Young's modulus of the material, surface tension, γ, will prevail and wipe out smaller features. These considerations can be put on firm analytical ground by a Fourier transform approach.

Consider a sinusoidal surface profile with amplitude h_0 and wavelength λ:

$$u_0 = h_0 \sin(2\pi x/\lambda)$$

Assuming $h_0 \ll \lambda$, the relaxed surface profile will still be sinusoidal with identical wavelength but reduced amplitude h_1. Thus, the surface displacement in the normal direction is

$$u = u_0 - u_1 = (h_0 - h_1)\ \sin(2\pi x/\lambda)$$

corresponding to the local pressure distribution[9]

$$p = \frac{\pi Y^*(h_0 - h_1)}{\lambda}\ \sin\left(\frac{2\pi x}{\lambda}\right)$$

where $Y^* = Y/(1 - \nu^2)$ and ν denotes Poisson's ratio. Thus, the elastic energy can be written as

* To whom correspondence should be addressed. Phone: +49(0)-2461613080. Fax: +49(0)-2461613907. E-mail: r.merkel@fz-juelich.de.

† IBN.

‡ IFF.

§ Present address: DWI e.V. and Institute of Technical and Macromolecular Chemistry, RWTH Aachen University, Pauwelsstrasse 8, 52056 Aachen, Germany.

(1) Whitesides, G. *Nature* **2006**, *442*, 368.
(2) Xia, Y.; Whitesides, G. *Annu. Rev. Mater. Sci.* **1998**, *28*, 153.
(3) Heyderman, L. J.; Schift, H.; David, C.; Gobrecht, J.; Schweizer, T. *Microelectron. Eng.* **2000**, *54*, 229.
(4) Chou, S. Y.; Krauss, P. R.; Renstrom, P. J. *Appl. Phys. Lett.* **1995**, *67*, 3114.
(5) Heidari, B.; Maximov, I.; Sarwe, E.; Montelius, L. *J. Vac. Sci. Technol.* **1999**, *17*, 2961.
(6) Hui, C. Y.; Jagota, A.; Lin, Y. Y.; Kramer, E. J. *Langmuir* **2002**, *18*, 1394.
(7) Rowland, H. D.; Sun, A. C.; Schunk, P. R.; King, W. P. *J. Micromech. Microeng.* **2005**, *15*, 2414.

(8) Ding, Y.; Ro, H. W.; Gerner, T. A.; Douglas, J. F.; Okerberg, B. C.; Karim, A.; Soles, C. L. *ACS Nano* **2007**, *1*, 84.

$$E_{el} = \frac{1}{2} \int d^2x u(x)\, p(x) = A_0 \frac{\pi Y^*}{4\lambda}(h_0 - h_1)^2$$

where A_0 is the nominal area of the surface. The surface energy is[10]

$$E_s = \gamma \int d^2x \left[1 + \left(\frac{du_1(x)}{dx}\right)^2 \right]^{\frac{1}{2}} \approx A_0 \gamma \left(1 + \frac{\pi^2 h_1^2}{\lambda^2} \right)$$

Minimizing the total energy $E_{el} + E_s$ with respect to h_1 gives

$$h_1 = \frac{h_0}{1 + 4\pi\gamma/(\lambda Y^*)} \tag{1}$$

In general, if the original surface profile is

$$h_0(x) = \int dq\, h_0(q) e^{iqx}$$

then using eq 1 (with $2\pi/\lambda = |q|$ and $r_0 = 2\gamma/Y^*$) we can obtain the modified or relaxed surface profile

$$h_1 = \int \frac{h_0(q) e^{iqx}}{1 + |q| r_0}\, dq \tag{2}$$

Applied to a step-like mold ($h_0(x) = d$ for $x < 0$, $h_0(x) = 0$ otherwise), this algorithm yields

$$h_1(x)/d = \begin{cases} 1 - f(-x/r_0)/\pi & \text{for} \quad x < 0 \\ f(x/r_0)/\pi & \text{else} \end{cases} \tag{3}$$

with the auxiliary function

$$f(t) = Ci(t)\sin(t) - Si(t)\cos(t) + \frac{\pi}{2}\cos(t) \tag{4}$$

This solution is also displayed in Figure 2. Here Ci denotes the cosine integral, and Si denotes the sine integral as defined in ref 11. Properties of the auxiliary function can be found in the same reference.

Because smoothing in Fourier space is a linear mathematical operation, the replica of a rectangular profile h_0 of height d and width $2b$ ($h_0 = d$ for $|x| < b$, zero otherwise) is given by the superposition of two edge profiles (eq 3), centered at $\pm b$. For our evaluations of microline samples as shown in Figure 1, we mostly used the height at the center, which is given by

$$\frac{h_1(0)}{d} = 1 - \frac{2}{\pi} f(b/r_0) \tag{5}$$

Materials and Methods

To test this model, Si/SiO$_2$ microstructures were prepared as described in ref 12 and used to mold the silicone elastomer, which, in the following text, is denoted as PDMS-E. The PDMS-E samples were prepared using a two-component kit (Sylgard 184) purchased from Dow Corning (Midland, MI) consisting of a base (vinyl-terminated polydimethylsiloxane) and a curing agent (methylhydrosiloxane-dimethylsiloxane copolymer) with a suitable catalyst. Mixtures of base and cross linker were prepared and poured over silanized silicon oxide molds patterned by optical lithography techniques. Glass coverslips were placed over the PDMS layers, and the whole ensembles were cured overnight at 60 °C. Two types of mold patterns were used. The first one consisted of a square lattice with 2.5 μm squares and a lattice constant of 3.5 μm (Figure 1a). The second one had long trenches of 2, 5, 10, and 20 μm width, with
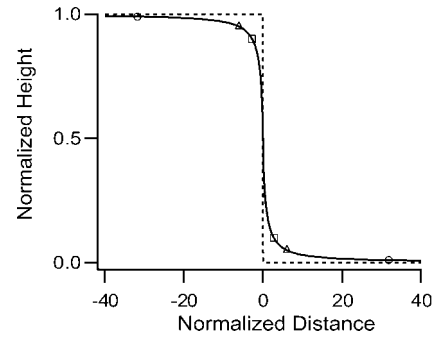
Figure 2. Calculated profile of the replica of an isolated step profile. Height is normalized by the step height, and distance is given in units of $r_0 = 2\gamma/Y^*$. The step is indicated by dotted lines. Also indicated are the points where the profile drops from 90 to 10% (squares, distance 5.48), from 95 to 5% (triangles, distance 12.2), and from 99 to 1% (circles, distance 63.5).

100 μm spacing in between (Figure 1d). A detailed description of the preparation of such samples can be found in ref 12.

The Young's moduli of PDMS-E were determined from stretching experiments[12] to an uncertainty of 10%. Because of significant variations in PDMS-E elasticity between different precursor batches, all line structures were prepared from a single batch. From this we prepared mixtures by weight of 10:1, 30:1, 35:1, 40:1, 45:1, 50:1, and 55:1 (base/cross linker) for which we obtained Young's moduli of 1.6 MPa and 144, 93, 48, 30, 17, and 11 kPa, respectively.

PDMS-E contains, besides the cross-linked silicone chains, some fraction of freely diffusing silicone oils. This is most pronounced at low cross-link densities where up to 30% of the material can be extracted by solvents such as isopropanol. Because oil extraction causes the samples to shrink by a difficult to control amount, we did not attempt to remove uncross-linked material. Because the cross-linked and the freely diffusing material are of very similar chemical nature and exhibit nearly identical surface free energies (20.3 mN/m for silicone oil and 19.9 mN/m for PDMS-E in air),[13] we do not expect strong variations in interface tension due to this freely diffusing fraction. This was indeed reported, albeit at higher cross-link density, in contact angle measurements of water on oil-extracted PDMS-E to which defined amounts of silicone oils had been added.[14]

Atomic force microscopy (AFM) images were acquired using a JPK NanoWizard (Berlin, Germany) instrument. Because the PDMS-E used in this study had an elastic modulus in the range of kPa, similar to the adhesives from Scotch tape or Post It notes,[15] the surfaces of these samples were very sticky. To prevent the adhesion of the tips to the samples, the scans were performed in aqueous detergent solutions (if not explicitly stated otherwise, 1% Triton X-100 from Sigma; some experiments were performed in 1% sodium dodecyl sulfate, SDS, from Sigma) in contact mode using Veeco cantilevers (spring constant 0.06 N/m). For samples with lines (Figure 1e,f), scan directions perpendicular to the lines were chosen. Under these conditions, the images were found to be identical in the forward and reverse scan directions.

Results and Discussion

As shown in Figure 1, scanning force microscopy demonstrated a substantial smoothing of microstructures molded in soft PDMS-E. We based our quantitative evaluation on microline samples because these allowed a straightforward comparison with theory. In the first step, we analyzed the heights of the

(9) Westergaard, H. *Trans. Am. Soc. Mech. Eng., J. Appl. Mech.* **1939**, *6*, 49.
(10) Zilberman, S.; Persson, B. *Solid State Commun.* **2002**, *123*, 173.
(11) Abramowitz, M.; Stegun, I. *Handbook of Mathematical Functions*; National Bureau of Standards: Washington, DC, 1964.

(12) Cesa, C.; Kirchgessner, N.; Mayer, D.; Schwarz, U.; Hoffmann, B.; Merkel, R. *Rev. Sci. Instrum.* **2007**, *78*, 034301.
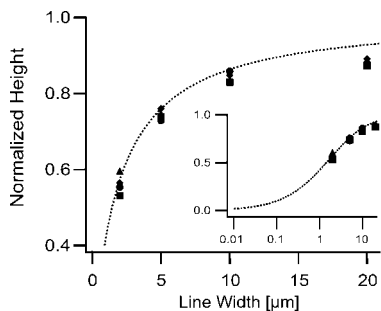(13) Wu, S. *Polymer Interface and Adhesion*; Marcel Dekker: New York, 1985.
(14) Kim, J.; Chaudhury, M. K.; Owen, M. J. *J. Colloid Interface Sci.* **2000**, *226*, 231.
(15) Peressadko, A. G.; Hosoda, N.; Persson, B. N. J. *Phys. Rev. Lett.* **2005**, *95*, 124301.

Figure 3. Heights of microlines molded in 11 kPa PDMS-E. Mold depths are 531 nm (circles), 299 nm (squares), 184 nm (triangles), and 93 nm (diamonds). The data are shown normalized by mold depth. The theory curve (dotted line) is eq 5 with $\gamma = 8.5$ mN/m. The inset shows the same data at different scaling.
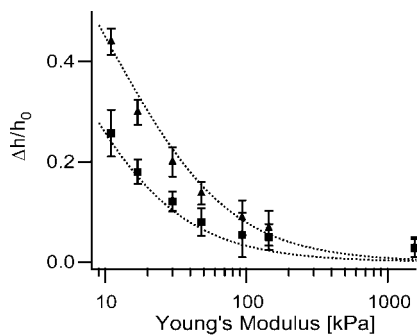

Figure 4. Normalized height change of the PDMS-E replicas produced in microline molds (Figure 1d) with depths of 531, 299, 184, and 93 nm. Error bars denote the standard deviation of the values measured at the different mold depths. Experimental results for line widths of 2 μm (triangles) and 5 μm (squares) are shown along with the theoretical results (eq 5), with an interface tension of 8.5 mN/m.

molded lines at their centers. As can be seen in Figure 3, these heights were proportional to the mold depth at otherwise identical parameters. Normalized heights (i.e., line heights divided by mold depths) of the different mold depths coincided on average to within 1.2%.

From the measured center heights of the lines, we calculated the interface tension γ at each data point by inverting eq 5. The smoothing effect was most pronounced for narrow lines in soft PDMS-E (cf. Figures 3 and 4). Accordingly, interface tensions retrieved from experiments under these conditions agreed well. This was also corroborated by an analysis of error propagation. To determine the interface tension, we used data taken under the following conditions: 2 μm width and all PDMS-E samples besides the stiffest one as well as 5 μm width and the four softest PDMS-E samples. From these data, we calculated a tension of 8.5 mN/m for the interface between PDMS-E and the Triton solution. The uncertainty was 1 mN/m. This interface tension resulted in smoothing lengths of r_0 ranging from 1.2 μm at 11 kPa stiffness down to 8 nm at 1.6 MPa. In view of substantial edge blurring of a soft replica (cf. Figure 2), the latter value agrees well with the maximum resolution obtainable with PDMS-E stamps in microcontact printing.[16]

Our interpretation of interface tension as a source of the smoothing effect is further supported by the marked influence of the type of detergent used. Identical samples prepared from 50:1 PDMS-E were imaged in two different detergent solutions, namely, 1% per weight sodium dodecyl sulfate (SDS) and 1%

(16) Schmid, H.; Michel, B. *Macromolecules* **2000**, *33*, 3042.
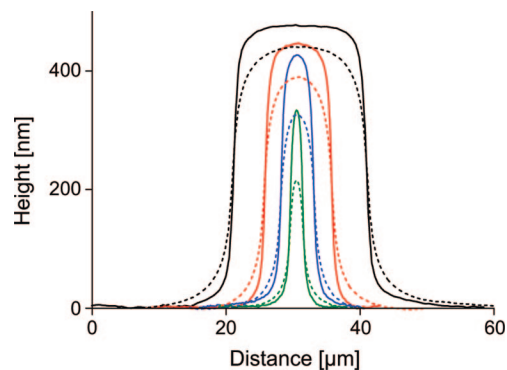
Figure 5. Height profiles of microlines of 50:1 PDMS-E produced in a mold such as that in Figure 1d with 531 nm depth. Continuous lines represent AFM contact mode scans in 1% Triton X-100, and dashed lines represent AFM contact mode scans in 1% SDS. Line widths are 20 (black), 10 (red), 5 (blue), and 2 μm (green).
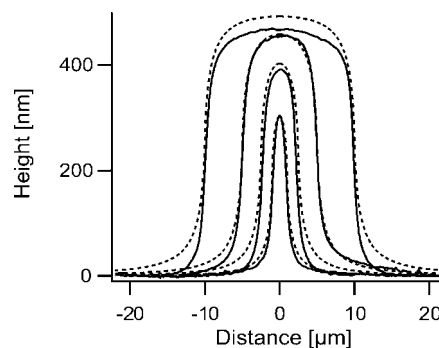
Figure 6. Measured (solid lines) and calculated (dashed lines) height profiles of lines molded in 11 kPa PDMS-E using 2-, 5-, 10-, and 20-μm-wide molds of 531 nm depth. Theory curves were calculated from eq 2 using an interface tension of 8.5 mN/m.

per volume Triton X-100. We found remarkably different results (cf. Figure 5). Ionic detergent SDS resulted in a higher degree of smoothing than did nonionic detergent Triton. Quantitative evaluation yielded a tension of 18 mN/m with an uncertainty of 3 mN/m for the interface between PDMS-E and the SDS solution. This value is 9 mN/m higher than the one measured in Triton X-100 solution.

Using an interface tension of 8.5 mN/m and the measured mechanical parameters of the PDMS-E samples, we calculated the expected profiles in Triton solution using eq 2 and a box profile for the mold (cf. Figure 6). Please note that the calculated profiles contain no adjustable parameters. Therefore, the agreement between theory and experiment for the 2- and 10-μm-wide lines molded in 11 kPa PDMS-E is indeed remarkable. As the profiles smoothly decayed to quite far distances, the determination of the baseline in scanning force micrographs faced its limit for the 20-μm-wide line. Here, height and shallow slopes were underestimated. Similar results were found for all other samples, albeit with less smoothing for stiffer PDMS-E.

In conclusion, we demonstrated experimentally and theoretically that the surface topography of samples prepared by replica molding strongly depends on the elasticity and surface tension of the material used in the molding process. This smoothing effect dominates replica shapes on the nanoscale (cf. Figure 3, inset). A careful analysis of the final shapes of

microstructures molded in soft PDMS-E of calibrated stiffness allows a quantification of the tension of the interface between elastomer and solution. Because the final shape of the replicas can be explicitly calculated using eq 2, one can take smoothing into account during mold design. For example, one could use molds with peaked edges and increased heights to compensate for the smoothing effects. This proposed strategy for improved soft lithography is similar to the approach in photolithography where light diffraction is compensated for during mask design.[17]

(17) Cole, D. C.; Barouch, E.; Conrad, E. W.; Yeung, M. *Proc. IEEE* **2001**, *89*, 1194.